Department of Pharmaceutics[1], Faculty of Pharmacy, Jamia Hamdard, Hamdard Nagar, New Delhi; Faculty of Pharmacy[2], Integral University, Lucknow (Uttar Pradesh), India; Department of Pharmaceutics[3], Faculty of Pharmacy, Al-Arab Medical University, Benghazi, Libya; New Drug Delivery Systems (NDDS)[4], Zydus Cadila Healthcare Ltd., Ahmedabad, Gujrat, India

Production, characterization, *in vitro* and *ex vivo* studies of babchi oil-encapsulated nanostructured solid lipid carriers produced by a hot aqueous titration method

M. Faiyazuddin[1,2], N. Akhtar[1], J. Akhter[2], S. Suri[1], F. Shakeel[3], S. Shafiq[4], G. Mustafa[1]

Received October 11, 2009, accepted October 23, 2009

Dr. Gulam Mustafa, Department of Pharmaceutics, Faculty of Pharmacy, Jamia Hamdard, Hamdard Nagar, New Delhi-110062, India
drmustafaghulam@gmail.com

Pharmazie 65: 348–355 (2010) *doi: 10.1691/ph.2010.9329*

An aqueous dispersion of solid fat nanoparticles of babchi oil (BO_{SLN}) was prepared by means of the hot water titration method. Surface morphology was determined by HR-TEM which revealed a fairly spherical shape of the formulations. Further they were evaluated for *in vitro* drug release characteristics and *ex vivo* skin permeation profile, zeta potential and particle diameter, rheological measures and droplet size distribution. Highest values for steady state flux (*J*ss), permeability coefficient (*K*p) and enhancement ratio (*E*r) were observed for formulation, **BO_{SLN}3** comprised of oil [10% v/v; BO (3.33%), CAT (6.67%)], Tween 80 (9.25% v/v), transcutol-P (28.75% v/v) and distilled water (53% v/v). These results suggest that the studied SLN might be promising vehicles for babchi oil in the management of psoriasis.

1. Introduction

Babchi oil (BO; *Psoralea corylifolia*) is a phytotherapeutic agent used in the treatment of psoriasis; having psoralen (photoactive furocoumarin) as a chief constituent that binds to DNA when exposed to UV light to form photoproducts with pyrimidine bases. Due to this action, babchi oil collectively inhibits DNA synthesis and causes decrease in cell proliferation (Farber and Nall 1974; Chang 2006).

Psoralen 7H-furo[3,2-g][I]benzopyran-7-one, is a tricyclic furocoumarin obtained from different species of Rutaceae, Umbelliferae, and Compositae families, and also synthesized commercially (Anderson and Voorhees 1980). In photochemotherapeutics, psoralens play a considerable role, particularly in skin disorders characterized by hyperproliferation, such as psoriasis (Farber and Nall 1974) which is effectively treated by means of PUVA therapy (psoralen-plus-UVA light). "P" in PUVA stands for psoralen, an oral drug that makes the skin much more light sensitive (Chang 2006). Modern photochemotherapy involves oral or topical administration of a photosensitizing psoralen followed by exposure to long-wavelength ($\leq$400 nm) UVA irradiation (Lowe et al. 1997). As aforesaid, psoralens are a group of compounds that bind to DNA in rapidly dividing cells and with ultraviolet light in the A band (UV-A) cause DNA cross-linking, thereby preventing cellular division (Hearst 1981; Musajo et al. 1967; Leite et al. 2004).

Novel strategies for topical drug delivery can play a vital role in psoriasis management by means of enhancing their dermal uptake with a concomitant reduction in their side effects (Asmussen 1991; Zouboulis 2004). In conventional dosage forms, *in vitro* experimental data obtained were very often followed by disappointing *in vivo* results, because of insufficient drug concentration due to poor absorption, metabolism, elimination, poor solubility and high fluctuation of plasma levels. A promising strategy to overcome these problems involves the development of novel drug carrier systems. In recent years, the attention of many researchers has focused on solid lipid nanoparticles (SLN) as alternative drug carriers to polymeric and liquid lipid nanoparticles, as it has many advantages over other colloidal carriers, e.g. regarding physical stability, protection of labile drugs from degradation, excellent tolerability and controlled release pattern. Lipophilic drugs (including babchi oil) have often been incorporated into SLNs for high drug loading and entrapment efficiency (Miglietta et al. 2000). Many methods have been developed to prepare SLNs, such as high pressure homogenization (Siekmann and Westesen, 1994; Lander et al. 2000; Lippacher et al. 2002, 2004), solvent emulsification or evaporation (Siekmann and Westesen, 1994) high speed stirring ultrasonication and solvent diffusion (Hu et al. 2005, 2006). Among the present encapsulation methods, high pressure homogenization (HPH) has been usually recognized as a reliable technique for SLNs preparation (Mehnert and Mader 2001). However, the drugs are susceptible to high shear stress and are destroyed during the formulation process (Perez et al. 2002). For the present study the microemulsion technique was selected to prepare the solid lipid nanoparticles (SLN). Therefore the aim of this study was to develop and evaluate lipidic nanocarrier loaded babchi oil (BO_{SLN}) by a hot water titrimetric method. This research paper focuses on the photo-chemotherapeutic

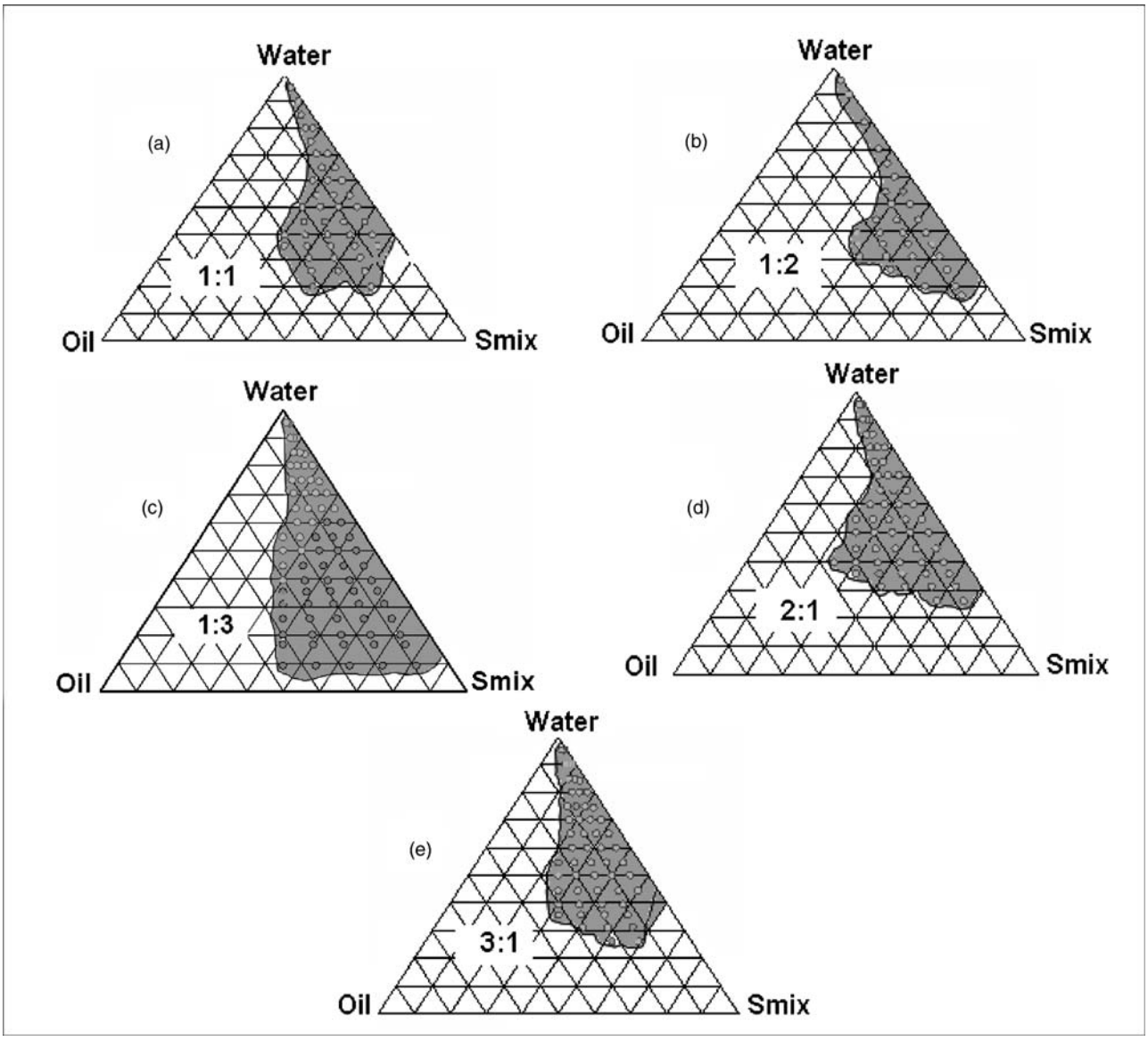

Fig. 1: Phase diagrams representing o/w nanoemulsion (shaded area) region of oil (BO: CAT; 1:2 v/v), surfactant (Tween 80), cosurfactant (Transcutol-P) at different S_{mix} ratios [Fig. 2a (S_{mix} 1:1), b (S_{mix} 1:2), c (S_{mix} 1:3), d (S_{mix} 2:1), e (S_{mix} 3:1)]

potential of a nanolipidic carriers system in the treatment of psoriasis by topical delivery of babchi oil.

2. Investigations, results and discussion

2.1. Screening of components

Babchi oil (BO) itself acts as a drug because it contains psoralen as an active component, already established for antipsoriatic activities (Anderson and Voorhees 1980; Farber and Nall 1974). Miscibility of the BO was determined in different solid fats. Miscibility studies were revealed that the drug was quite miscible (even after cooling; $\leq 8\,^{\circ}C$) with CAT, cetyl alcohol and glyceryl monostearate. By comparing the phase behaviour of lipidic mixtures (BO:solid fat: 1:2), the result was obvious with Compritol 888 ATO (CAT) (Table 1). On this basis of the above findings CAT was selected as an external solid medium for the lipid core of BO. Phasic behavior of BO was also determined in different S_{mix} combinations, as secondary parameters for the screening. The defined phasic surface area for BO is given in Table 1; as Tween 80 (305.52 ± 2.74) > Tween 20 (258.21 ± 2.75) > Cremophor EL (112.42 ± 2.32) > Transcutol P (95.32 ± 2.82) > Labrasol (85.53 ± 2.48) > ethanol (74.32 ± 2.02) > Labrafil (69.13 ± 1.16) > Plurol oleique (62.32 ± 2.01). Maximum phasic area was appeared for Tween 80 (Surf) and Transcutol-P (CoS) (Table 1). Therefore, Tween 80 and Transcutol-P were selected as surfactant and

Table 1: Comparative phasic behavior of babchi oil in various surfactants and co surfactants

Component	Surface area ± SD (cm^2)
Labrafil	69.13 ± 1.16
Labrasol	85.53 ± 2.48
Cremophor EL	112.42 ± 2.32
Tween 80	305.52 ± 2.74
Tween 20	258.21 ± 2.75
Ethanol	74.32 ± 2.02
Tanscutol P	95.32 ± 2.82
Plurol oleique	62.32 ± 2.01

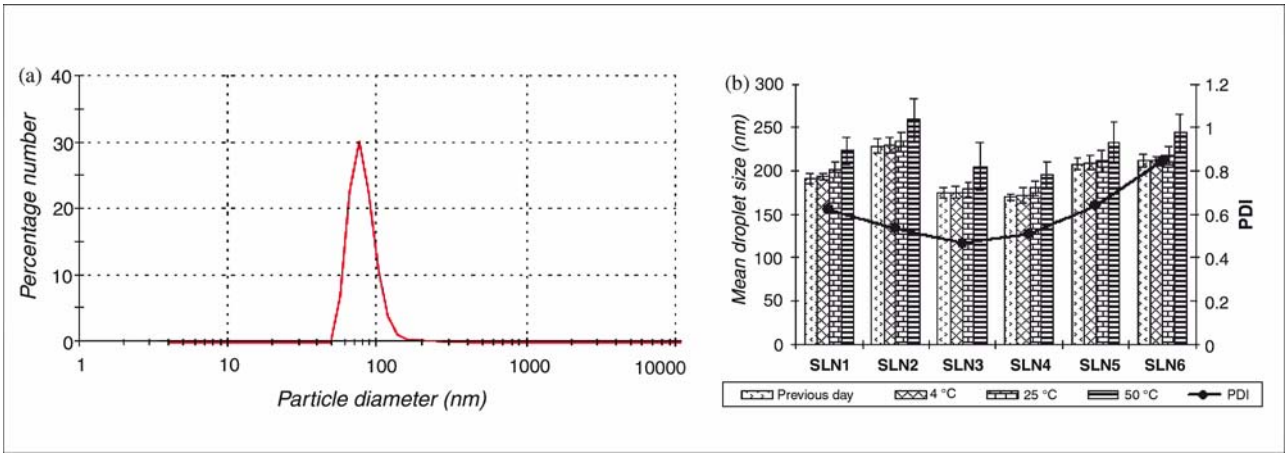

Fig. 2: Babchi oil-SLN formulation characterized for (a) particle size distribution and (b) particle growth analysis with polydispersity index at different temperatures

cosurfactant mixtures (S_{mix}) in the development of SLN formulations.

2.2. Phase studies for babchi oil

Pseudoternary phase diagrams were constructed using a microemulsion technique at a constant temperature of 25 ± 0.5 °C. Full attention was taken in order to ensure that observations were not made on metastable systems, although the free energy required to form an emulsion is very low, the formation is thermodynamically spontaneous (Craig et al. 1995). Pseudoternary phase diagrams were constructed separately for each S_{mix} ratio (Fig. 1a–e), so that O/W nano-regions could be identified for the optimization of SLNs. S_{mix} ratio of 3:1 (Fig. 1c) had a larger nanophasic region compared to the other S_{mix} ratio (Fig. 2a–b & d–e). O/W solid nanoemulsion region was appeared towards the aqua rich apex of the phase diagram with higher concentration of S_{mix}, showing that Tween 80 could be used alone without cosurfactant, but liquid crystalline form (S_{mix}: 1:2 < 1:1 < 2:1 < 3:1) limits its implication and therefore it was advised to use a co-surfactant to cope up the rigid crystalline interface. From the phase diagram, it was observed that S_{mix} 1:0 (Figure not shown), was not capable of breaking the interfacial tension on the oil surface; and more liquid crystalline (LC) area appeared in the phase diagram. But in case of S_{mix} 1:1 (Fig. 1a), when cosurfactant was mixed with a surfactant, the interfacial film emerged more flexible and less LC area appeared than in the previous case when Tween 80 was used alone (S_{mix} 1:0). The maximum concentration of lipid that was solubilized in the phase diagram (Fig. 1a) was nearly 35 ± 1.31% v/v by incorporating S_{mix} around 62 ± 3.14% v/v, what showed the supremacy of Tween 80 in nanosizing. It was observed that increasing the concentration in S_{mix} ratio (S_{mix} 1:1 - 1:3; Fig. 1a–c), a marked decline in liquid crystals appeared and a proportionate augment in the nanophasic region occurred. However on increasing the surfactant concentration in S_{mix} ratios (S_{mix} 2:1-3:1; Fig. 1d–e); a significant increase in liquid crystals and a substantial decrease in the nanoemulsion region was observed. Perhaps, this is due to a further drop in interfacial tension and increase in fluidity at interface; leading to a slight increase in entropy of the system; following more incorporation of BO in the hydrophobic region of the surfactant monomers (Lawrence and Rees 2000). The exaggeration in the nanophase system was insignificant when surfactant concentration in S_{mix} was increased from 2:1 (Fig. 2d). Possibly, this is a LC phase generated by Tween-80 and it was not appeased by the present amount of co-surfactant. These findings reveal that free energy of nanoemulsion formation is somehow dependent on the extent to which the surfactant and co-surfactants compliantly lower the surface tension of the oil-water interface and the change in dispersion entropy (Lawrence and Rees 2000; Craig et al. 1995). In such a case solid NE formation is spontaneous and the resulting dispersion is physically stable (Baboota et al. 2007). When the S_{mix} ratios (2:1 and 3:1) were studied, not any further increase in nanoemulsion area was observed and liquid crystalline area started coming in diagrams, probably due to increased participation of surfactant (Fig. 1d–e). For our interest those formulations were selected from each pseudoternary phase diagram, in which amount could accommodate optimum quantity of oil phase by using lowest possible S_{mix}.

2.3. Formulation development

Considering pseudoternary phase diagrams, maximum regions were shown by a S_{mix} ratio of 1:1, 1:2 and 1:3. Other combinations of S_{mix} were also constructed but not taken into account because they have shown very tiny nanophasic regions compared to LC forms. Solid nanoemulsion formulations with different formulas from phase diagrams were selected on the evidence based performance of different thermodynamic stability studies. Almost the entire range of nanoemulsion occurrence in the phase diagrams was covered and different lipid compositions with minimum surfactant concentration showing nanoemulsion existence were precisely selected (Table 2). The oil (BO: CAT: 1:2) was taken and the required amount of S/CoS was added in the prescribed ratio with drop-wise hot water addition until a clear and transparent solution was obtained, which was later on solidified by addition of chilled water.

2.4. In vitro thermodynamic stability test

Solid nanoemulsions are physically and thermodynamically stable systems and are formed at a particular concentration of oil (solid fat), surfactant (S_{mix} ratio) and water (external phase), with no phase separation, creaming or cracking (Shafiq et al. 2007a). For the sake of optimization of stable and robust formulations, the selected preparations were subjected to different physical stability tests (centrifugation, heating-cooling cycle and freeze-thaw cycle). Those formulations, which survived *in vitro* physical stability tests, were taken for further studies. The compositions of these formulations are depicted in Table 3. The criteria for optimization of SLN from these selected formulations were based on composition having lower S_{mix} concentration and high lipid content. Formulation composition having 5% v/v of lipid shows excellent transparency but the quantity of BO was too low for getting therapeutic potential.

Table 2: Thermodynamic stability screening of BO-SLN formulations

Oil: Babchi oil + Compritol 888 ATO (1:2 v/v), Surfactant: Tween 80, Cosurfactant: Transcutol-P, external phase: distilled water

S_{mix} Ratio (S:CoS)	*S. No.*	*Percentage v/v of different components in formulations*			*Observations based on the thermodynamic stability studies*			*Inference*
		Lipid	S_{mix}	Water	H/C	Cent	Freeze	
1:0	1	5	30	65	√	√	√	Passed
	2	5	38	57	√	√	√	Passed
(Not shown)	3	10	39	51	√	x	–	Failed
	4	10	40	50	√	√	–	Failed
	5	15	40	50	√	x	–	Failed
	6	5	31	64	√	√	√	Passed
	7	5	40	55	√	√	√	Passed
1:1	8	10	39	51	√	√	√	Passed
	9	10	42	48	√	√	√	Passed
(Fig. 1a)	10	15	40	50	x	–	–	Failed
	11	5	37	58	√	√	√	Passed
	12	5	40	55	√	√	√	Passed
1:2	13	10	45	45	√	x	–	Failed
	14	10	46	44	√	√	√	Passed
(Fig. 1b)	15	15	48	37	x	√	√	Failed
	16	5	37	58	√	√	√	Passed
	17	5	40	55	√	√	√	Passed
1:3	18	10	37	53	√	√	√	Passed
	19	10	41	49	√	√	√	Passed
(Fig. 1c)	20	15	44	41	x	–	–	Failed
	21	5	35	60	√	√	√	Passed
	22	5	40	55	√	√	√	Passed
2:1	23	10	41	49	√	√	√	Passed
	24	10	42	48	√	√	√	Passed
(Fig. 1d)	25	15	40	45	x	√	√	Failed
	26	5	40	55	√	√	√	Passed
	27	5	56	39	√	√	√	Passed
3:1	28	10	39	51	√	√	√	Passed
	29	10	50	40	√	√	√	Passed
(Fig. 1e)	30	15	45	40	√	√	x	Failed

H/C: Heating and cooling (0 °C and 45 °C); Cent: Centrifugation (5000 rpm); Freeze: Freeze-thaw (−21 °C and +25 °C)

This concept was led to increase the dose size of the formulation. Therefore all the formulation having at least 10% v/v of the lipid composition was screened for the proposed study (Table 3).

2.5. Characterization and optimization of solid lipid nanoparticles

2.5.1. Entrapment efficiency

A high amount of BO could be incorporated in the SLN, as shown in Table 4. As the drug is itself an oil (BO), with highest miscibility in CAT could be expected to get entrapment up to 100% with respect to the lipid integrated. The percentage of incorporated drug in the lipid matrix (entrapment efficiency) was evaluated over a period of one month. The amalgamation of BO with CAT led to high entrapment efficiency i.e., $68.32 \pm 9.06\%$ ($BO_{SLN}1$); $69.72 \pm 11.6\%$ ($BO_{SLN}2$); $70.12 \pm 7.76\%$ ($BO_{SLN}3$); $67.53 \pm 8.16\%$ ($BO_{SLN}4$); $72.83 \pm 12.5\%$ ($BO_{SLN}5$) and $68.83 \pm 12.4\%$ ($BO_{SLN}6$), probably because of their lipophilic character and better loading capacity in stabilized formulations. This is because of the binary mixture of liquid and solid lipids, resulting in less ordered recrystallization (Jenning et al. 2000).

2.5.2. Particle diameter and surface charge analysis

The size distribution and surface charge analysis were performed for selected formulations by Malvern Zetasizer (Nano ZS-90, UK). The statistical distribution of droplet size is shown in the Fig. 2. Table 4 summarizes mean droplet

Table 3: Composition of selected BO-SLN that passed the physical stability tests (%v/v)

Formulation Code	Percentage composition of selected formulation			S_{mix} ratio
	Oil	S_{mix}	Water	
BO_{SLN1}	10	42	48	1:1
BO_{SLN2}	10	46	44	1:2
BO_{SLN3}	10	37	53	1:3
BO_{SLN4}	10	41	49	1:3
BO_{SLN5}	10	42	48	2:1
BO_{SLN6}	10	39	51	3:1

Table 4: Intrinsic and extrinsic properties of optimized SLN formulations (n = 3)

Code	% $E_E \pm$ sd	% $D_R \pm$ sd	$R_I \pm$ sd	$\Delta_{dm} \pm$ sd (nm)	p_i	$\zeta \pm$ sd (mV)	$\eta \pm$ sd (cps)
BO_{SLN1}	68.32 ± 9.06	58.46 ± 5.29	1.364 ± 0.006	191.8 ± 6.08	0.621	20.31 ± 4.8	136.42 ± 6.97
BO_{SLN2}	69.72 ± 11.6	49.34 ± 7.12	1.360 ± 0.007	228.6 ± 5.99	0.537	23.6 ± 4.8	127.31 ± 8.17
BO_{SLN3}	70.12 ± 7.76	64.97 ± 8.56	1.358 ± 0.008	174.8 ± 7.95	0.267	25.2 ± 1.98	119.45 ± 6.83
BO_{SLN4}	67.53 ± 8.16	62.46 ± 11.81	1.364 ± 0.011	169.4 ± 4.98	0.311	28.28 ± 2.68	121.51 ± 8.97
BO_{SLN5}	72.83 ± 12.5	53.06 ± 3.31	1.365 ± 0.010	208 ± 3.53	0.638	34.4 ± 3.76	153.45 ± 7.72
BO_{SLN6}	68.83 ± 12.4	49.06 ± 3.31	1.366 ± 0.010	212 ± 6.18	0.843	32.5 ± 2.36	167.24 ± 8.17

Entrapment efficiency (E_E); Drug release in 24 h (D_R); Refractive index: (R_I); Average particle diameter (Δ_{dm}), Polydispersity index (p_i); Zeta potentials (ζ) Viscosity mean (η)

size of optimized formulations ($BO_{SLN}1$-$BO_{SLN}6$) ranging from 169–228 nm. Largest droplet size appeared in $BO_{SLN}2$, which may be ascribable to the presence of higher concentrations of surfactants (Table 3) leading to formation of rigid interfacial tension. An inadequate amount of co-surfactant was unable to provide further flexibility to the rigid film for the secondary nanosizing. Droplet size analyses of the selected formulations showed that the size increased with increase in the concentration of oil and S/CoS ratio. The polydispersity value (PI) was found <1 for all formulations indicating narrow distribution. $BO_{SLN}3$ claimed least PI value (0.2671) suggesting uniformity in droplet size.

Generally it is accepted that ZP values of 30 mV and above characterize a stable formulation. $BO_{SLN}5$ formulation had highest ZP (34.4 ± 3.76 mV) on day one, which did not significantly change after one month for all storage temperatures (Table 5) indicating long-term stability. On day one, $BO_{SLN}1$-$BO_{SLN}6$ formulations showed a ZP value of 20 to 34 mV, which was slightly increased after 90 days (room temp: 25 °C and 4 °C storage temperature) (Table 5). $BO_{SLN}1$-$BO_{SLN}6$ when stored at 50 °C showed the lowest average value of ZP (14.9 to 28.2 mV) with radical change in particle size (Table 5). The values obtained at higher temperatures are supported by an investigation carried out by Freitas and Muller (1998), evaluating the effect of light and temperature on zeta potential and physical stability in SLN dispersions using poloxamer as a stabilizer. Consequently it can be inferred that at high temperature (50 °C), the steric stabilizing property of Tween 80 was not sufficient enough leading to particle agglomeration.

2.5.3. Rheological measures

Table 4 reports viscosity data of optimized formulations ($BO_{SLN}1$-$BO_{SLN}6$) ranging from 119.45-167.24 cps. The viscosity results can be correlated with the different contribution of the surfactants as well as co-surfactant consumed in stabilization of selected formulation composition. The viscosity of the formulation $BO_{SLN}3$ was lowest (119.45 ± 6.83 cps) as compared to other formulations, making apposite for cosmeceutical use. The low viscosity value in terms of desired rheological measure is perhaps due to the integration of mere quantity of surfactant rather than oil concentration (as all formulations have fixed oil quantity).

2.5.4. In vitro release studies of BO-SLN

Optimized SLNs were investigated for *in vitro* release pattern using a dialysis membrane over Franz diffusion cell (Jayaraman et al. 2009) with an effective diffusion surface area of 7.16 cm^2 and 37 ml of receiver capacity. Dialysis membrane (Hi-Media, Mumbai, India) having a pore size of 2.4 nm, and a molecular weight cut-off between 12000–14000 was used. Studies were performed to compare the release of drug from different selected formulations and neat BO. The release of drug from SLN was extremely significant ($p < 0.01$) when compared to neat BO (Table 4). Drug release from $BO_{SLN}3$ was very rapid, as 64.97 ± 8.56% of drug was released in 24 h. While other formulations showed a comparatively slow release pattern [$BO_{SLN}3$ (64.97 ± 8.6%) > $BO_{SLN}4$ (62.46 ± 11.8%) > $BO_{SLN}1$ (58.46 ± 5.3%) > $BO_{SLN}5$ (53.06 ± 3.3%) > $BO_{SLN}2$ (49.34 ± 7.1%) > $BO_{SLN}6$ (49.06 ± 3.3%)] in 24 h. In contrast to optimized SLNs, neat BO was found extremely low (30% in 24 h). SLN formulations have smaller particle size providing larger surface area for rapid dissolution prerequisite (justified by droplet size distribution) (Fig. 2).

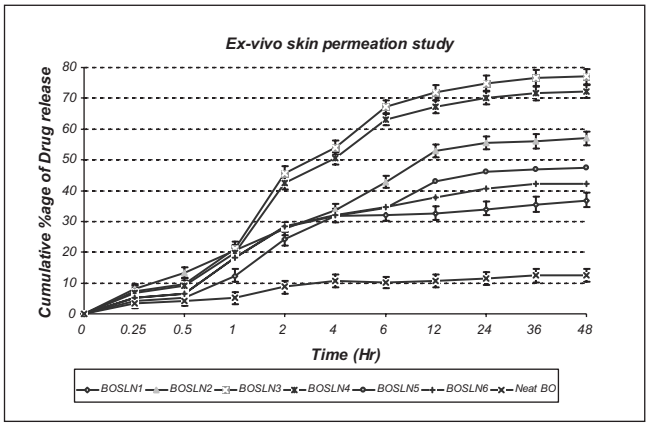

Fig. 3: *Ex vivo* skin permeation profile of BO in SLN dispersions, (n = 3)

2.5.5. Ex vivo skin permeation studies

Ex vivo skin permeation studies were performed to compare the permeation pattern of BO from optimized SLN formulations and neat BO. In order to maintain the sink condition, acetate buffer (pH 5.4) was added along with ethanol (20% v/v) in the receiver compartment of the cell. *Ex vivo* skin permeation was highest for $BO_{SLN}3$ and lowest in neat BO (Fig. 3). Maximum release was shown in $BO_{SLN}3$, perhaps due to its least droplet size and lowest viscosity as compared to other formulations ($BO_{SLN}3 > BO_{SLN}4 > BO_{SLN}5 > BO_{SLN}2 > BO_{SLN}6 > BO_{SLN}1 >$ neat BO). The possible mechanism by which solid lipid nanoparticles enhance the skin permeation of drugs is the lipid pathway of the stratum corneum, in which neutral lipids are arranged as bilayers with their hydrophobic chains facing each others to form a lipophilic bimolecular leaflet (Zouboulis 2004) and the drug dissolved from the lipid domain of SLN to directly penetrate into the stratum corneum, thereby destabilizing its bilayer structure with the help of surfactant present. On the other hand its hydrophilic domain deeply hydrates the stratum corneum, preferably important in the percutaneous drug uptake

Table 5: Zeta potential and mean particle size of SLNs measured on day 1 and day 90 of storage at different temperatures

Code	Previous day sampling		90th day sampling					
	$\Delta_{dm} \pm sd$ (nm)	$\zeta \pm sd$ (mV)	4 °C		25 °C		50 °C	
			$\Delta_{dm} \pm$ sd (nm)	$\zeta \pm$sd (mV)	$\Delta_{dm} \pm$ sd (nm)	$\zeta \pm$sd (mV)	$\Delta_{dm} \pm$ sd (nm)	$\zeta \pm$sd (mV)
BO_{SLN1}	191.80 ± 6.08	20.31 ± 4.8	193.56 ± 0.29	20.89 ± 6.3	201.50 ± 2.48	17.45 ± 2.78	223.25 ± 3.12	14.91 ± 1.5
BO_{SLN2}	228.61 ± 5.99	23.60 ± 4.8	230.12 ± 0.29	24.52 ± 6.3	233.41 ± 0.92	21.59 ± 1.25	258.31 ± 0.19	19.65 ± 2.23
BO_{SLN3}	174.80 ± 7.95	25.21 ± 1.98	175.33 ± 0.51	25.81 ± 2.19	178.41 ± 0.19	21.91 ± 3.24	204.84 ± 1.18	17.21 ± 0.94
BO_{SLN4}	169.41 ± 4.98	28.28 ± 2.68	171.47 ± 0.21	28.55 ± 3.26	179.40 ± 0.38	24.62 ± 3.14	194.83 ± 1.08	19.48 ± 0.65
BO_{SLN5}	208.08 ± 3.53	34.40 ± 3.76	209.23 ± 2.23	34.61 ± 2.68	211.71 ± 1.03	31.22 ± 4.32	232.51 ± 1.33	25.12 ± 1.6
BO_{SLN6}	212.10 ± 6.18	32.51 ± 2.36	211.13 ± 2.23	32.78 ± 3.72	217.41 ± 1.03	30.71 ± 2.32	243.71 ± 2.43	28.19 ± 2.56

(Baboota et al. 2007). BO is lipophilic by nature; therefore it permeates more easily through the established lipid pathway; however when surfactant is integrated normally in production of SLNs, permeation cascade gets synergized. Therefore, small droplet size and low viscosity range of SLN makes it an outstanding carrier for enhanced percutaneous uptake.

Permeability parameters like steady state flux (*J*ss), permeability coefficient (*K*p) and enhancement ratio (*E*r) were significantly increased in SLNs as compared to neat BO ($p < 0.05$). The most perceptible grounds for enhanced permeation of babchi oil from $BO_{SLN}3$ could be the combined effects attributed due to Tween 80 and Transcutol-P (due to nanosizing) and lowest rheological measures. Permeability parameters of different SLNs and neat BO are depicted in Table 6.

2.5.6. *Effect of storage temperature*

To study the effect of temperature on particle size, all the optimized formulations were kept in colorless and transparent glass vials and exposed to different stress temperatures (4 °C, 25 °C and 50 °C) for a minimum period of 90 days. A minute increase in particle size was observed at 4 °C and 25 °C storing conditions. However, a significant growth in particle size was monitored nodes high temperature storage conditions (≥50 °C). Mean particle diameter of the $BO_{SLN}3$ stored at 50 °C was increased from 174.80 to 204.84 nm in 90 days, whereas 175.33 nm and 178.41 was observed when stored at 4 °C and 25 °C respectively (Table 5). The result strongly supports the protecting ability of Tween-80 at moderate temperatures. Similar results were predicted in the case of others formulations (size: 50 °C > 25 °C > 4 °C). These results also corroborate with zeta potential data obtained for samples stored at different temperatures (Table 5). From the above findings it can be inferred that the particle aggregation process accelerated with the increase in storage temperatures. This is perhaps due to the destabilization of the physically critical SLN dispersions as a consequence of input energy provided by the successively higher temperatures. This energy input increases the kinetic energy of the particles and favors their collision, resulting in particle aggregation. Another reason could be the change in performance of the surfactant film on the particle surface with temperature. The constant changes in polymorphic modifications of the lipid particles with time, results in an increase in the particle surface area due to preferred formation of platelet-shaped particles characteristic of the β-modification. The surfactant molecules can no longer give sufficient coverage to the newer surfaces formed resulted in particle growth.

In conclusion, on the basis of higher drug permeation, lowest droplet size, minimum polydispersity, lowest viscosity, optimum surfactant and cosurfactant concentration, better drug release profile and enhanced *ex vivo* skin permeation profile, $BO_{SLN}3$ was optimized as a solid lipid nanoparticle formulation, comprised of oil [10% v/v; BO (3.33%), CAT (6.67%)], Tween 80 (9.25% v/v), Transcutol-P (28.75% v/v) and distilled water (53% v/v) carrier for topical preparations. After 90 days of storage at different temperatures the mean diameters and zeta potential of SLN remain practically the same, which emphasizes the physical stability of these nanolipidic carriers. From *in vitro* results it can be concluded that the developed SLN might be a promising vehicle for improved topical delivery of babchi oil in the treatment of psoriasis.

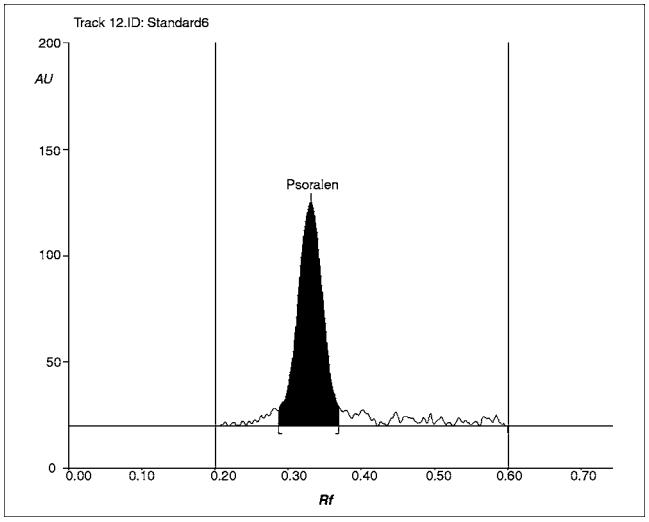

Fig. 4: A typical chromatogram of psoralen (chief constituent of babchi oil) with R_f value of 0.32 at λ_{max} of 250 nm

3. Experimental

3.1. Materials

Babchi oil was purchased from Aroma House, New Delhi, India. Tween 80 and Tween 20 were purchased from CDH, Mumbai, India. Psoralen was purchased from Sigma-Aldrich Chemicals Private Limited., India. Compritol 888 ATO, which was obtained from Gattefossé (Weilam Rhein, Germany), is declared as glycerol behenate with a melting point of 72 °C. Transcutol-P (diethylene glycol monoethyl ether), Cremophor-EL (polyoxy-35-castor oil), Labrasol (caprylocaproyl macrogolglycerides), Labrafil (linoleoyl macrogolglycerides) and Pleurol oleique (polyglycerol oleate) were gift samples from Gattefosse (Saint Priest, Cedex, France). CAT and ethanol were purchased from E. Merck, Mumbai, India. Water was obtained from a Milli-Q water purification system (Millipore, Billerica, MA).

3.2. Analytical methodology

BO was analyzed by previously established high performance thin-layer chromatographic method for psoralen (Ali et al. 2008), as it is the chief constituent of this oil (Fig. 4). The chromatographic estimation was performed with a *CAMAG* microlitre syringe on precoated silica gel aluminum plate $60F_{254}$ using *CAMAG* Linomat V sample applicator (*CAMAG*, Muttenz, Switzerland). The mobile phase optimized was

Table 6: *Ex vivo* permeability parameter of different BO-SLNs and neat BO ($n = 3$)

Matrices	Flux ($Jss \pm sd$; mg/cm^2/h)	Permeability constant ($Kp \pm sd$; cm/h $\times 10^{-2}$)	Enhancement Ratio (Er)	p-value†
Neat BO	0.0447 ± 0.0045	0.0267 ± 0.20	–	–
BO_{SLN1}	0.2056 ± 0.0024	0.8224 ± 0.19	4.59	>0.01
BO_{SLN2}	0.2253 ± 0.087	0.9012 ± 0.11	5.04	<0.01
BO_{SLN3}	0.2871 ± 0.085	1.1484 ± 0.14	6.42	<0.01
BO_{SLN4}	0.2681 ± 0.012	1.0724 ± 0.14	5.99	>0.05
BO_{SLN5}	0.2539 ± 0.010	1.0156 ± 0.16	5.68	<0.05
BO_{SLN6}	0.2215 ± 0.065	0.8860 ± 0.15	4.95	<0.05

† p-value (Neat BO v/s BO-SLNs)

n-hexane–acetone–formic acid 8:4:0.1 (v/v/v). A compact, resolved psoralen peak (R_f value 0.32 ± 0.02) was observed by densitometric analysis in absorbance mode at 250 nm. All the BO-SLN formulations were analyzed by this method for *in vitro* release as well as for permeation profile.

3.3. Constructing the map of the nanoemulsion-phase

In order to find out the concentration range of various components for the existence range of nanolipid carrier, pseudoternary phase diagrams were constructed using microemulsion technique. The oil (BO) was premixed with the solid fat [Compritol 888 ATO (CAT)] after melting on hot water bath and combination of Tween 80 and Transcutol-P was used as surfactant and cosurfactant, respectively. Distilled water (maintained at water bath) was used as an external aqueous media for titration. Surfactant and cosurfactant (S_{mix}) were pre-mixed in different volume ratios (1:0, 1:1, 1:2, 1:3, 2:1, 3:1, 4:1). These S_{mix} ratios were chosen in increasing concentration of cosurfactant with respect to surfactant and increasing the concentration of surfactant with respect to cosurfactant for comprehensive study. For each phase diagram, oil phase [Babchi oil (BO): Compritol 888 ATO (CAT): 1:2] and specific S_{mix} ratio was mixed thoroughly in different volume ratios from 1:9–9:1 in different glass vials. Slow titration with aqueous phase (hot water) was done for each combination of oil and S_{mix} separately (Baboota et al. 2007; Shafiq et al. 2007). The physical state of the solid nanoemulsions was marked on a pentameric component based phase diagram with one axes representing the aqueous phase, oil phase (BO and CAT mixture) and the third representing a mixture of surfactant and cosurfactant at fixed volume ratios (S_{mix} ratio).

3.4. Formulation development

SLN have been formulated as detailed by Muller and Lucks (1996) with small modification; therefore from the pseudoternary phase diagram, nanolipidic regions were mapped out and diverse formulations from this location were selected for study. This pre-emulsion [nanolipidic droplets (NLD)] was subsequently recrystallized upon cooling with the chilled water maintained at 6–8 °C with continuous stirring. To get the normal size distribution, obtained formulation was stirred constantly (45 min) using a magnetic stirrer.

3.5. Characterization and optimization of solid lipid nanoparticles

3.5.1. Thermodynamic stability test

To overcome the problem of metastable formulation, thermodynamic stability tests were performed (Li et al. 2005; Shafiq et al. 2007a, b). Screened formulations were further centrifuged (5000 rpm; 30 min) and observed for physical changes (phase separation, creaming or cracking). Formulations with no phase separation were further considered for heating and cooling cycle (Six cycles; Temp: 0 °C–45 °C; 48 h for each either heating or cooling). Those formulations, which survived these stress temperatures, were subjected to freeze thaw (Six cycles; Temp: −21 °C to 25 °C; 48 h for each either freeze or thaw) (Table 2).

3.5.2. Entrapment efficiency

Entrapment efficiency (EE %) is expressed as the percentage of the total amount of BO found in the studied formulations at the end of the preparation procedure. The SLN dispersions were purified from non incorporated BO traces by repeated washing. The encapsulation efficiency was calculated using the following equation: $[(Q_t\text{-}Q_S)/Q_t] \times 100$.
Where 'Q_t' is the total quantity of incorporated and non-incorporated oil in the SLN dispersion and 'Q_S' is the non-incorporated oil quantity. Quantitative determination was performed by HPTLC (*CAMAG*, Muttenz, Switzerland) by using n-hexane–acetone–formic acid [2: 1: 0.025 (v/v/v)] as mobile phase at 250 nm in absorbance mode (Ali et al. 2008). The entrapment efficiency of BO-loaded SLN (BO_{SLN}) is shown in Table 4.

3.5.3. Particle diameter and surface charge analysis

Particle diameter was determined using a photon correlation spectrometer (PCS; Zetasizer-1000 HAS, Malvern Instruments, UK) based on the laser light scattering phenomenon, which analyzes the fluctuations in light scattering. Light scattering was monitored (25 °C; Angle: 90°). Properly diluted samples of SLN (0.1 mL) were dispersed in 50 mL of distilled water and were used for particle size analysis. Average particle diameter (Δ_{dm}), polydispersity index (p_i) and zeta potentials (ζ) were recorded.

3.5.4. Rheological measures

Rheological measures were performed for the optimized formulations on Brookfield DV III ultra V6.0 RV cone and plate viscometer (Brookfield Engineering Laboratories, Inc, Middleboro, MA) using spindle # CPE40 at 25 ± 0.3 °C). All measurements were carried out at a temperature of 25 ± 0.5 °C. The software used for the calculations was Rheocalc V2.6.

3.5.5. In vitro release studies of BO-SLN

The optimized formulations were investigated for *in vitro* drug release; using dialysis bag method fitted in Franz diffusion cell (diffusion surface area: 7.16 cm^2; volume: 37 ml of receiver chamber) (Jayaraman et al. 2009). Dialysis membrane (pore size: 2.4 nm, MW: 12000–14000 Da) was soaked in double distilled water for 12 h before mounting in a Franz diffusion cell. The release profile in phosphate buffer with pH 5.6 was also used as to simulate the skin pH. BO_{SLN} dispersion (≈1 mL) was placed in the donor compartment and the receptor compartment was filled with dissolution media (12 mL). During the experiments, the solution in receptor side was maintained at normal conditions (temp: 37 °C ± 0.5 °C; 800 rpm). Samples (100 µL) were of the withdrawn from the receiver compartment through a side tube at a regular time intervals (0, 0.5, 1, 1.5, 2, 4, 6, 8, 10, 12, 24, 36 and 48 h) and the volumes withdrawn were replaced with the fresh media each time. The release of drug from formulation was compared with the neat BO. The samples were analyzed for the drug content using developed HPTLC method at 250 nm. Statistical analysis was performed by one way analysis of variance (ANOVA) using Dunnett test using Graph-Pad Prism version 4.0 (San Diego, CA, USA).

3.5.6. Ex vivo skin permeation studies

Ex vivo skin permeation studies were performed using a Franz diffusion cell with an effective diffusion surface area of 7.16 cm^2 and 37 ml of receiver chamber capacity using excised rat abdominal skin. The cleaned skin was washed with distilled water and stored in the deep freezer at −21 °C until further use. The skin was brought to room temperature and mounted between donor and receiver compartment of the Franz diffusion cell; the *stratum corneum* side was facing the donor compartment and the dermal side was facing the receiver compartment and stabilized with the dissolution medium. For this, the receiver chamber was filled with ethanolic acetate buffer pH 5.4 (9:1) and stirred with a magnetic rotor at a speed of 100 rpm in a hot air oven maintaining temperature at 37 ± 1 °C. The whole ethanolic acetate buffer was replaced with a fresh one after every 30 min to stabilize the skin. After running the 12 cycle of stabilization, 1 mL SLN formulation of BO was placed into donor compartment. The samples were withdrawn at regular interval (0.5, 1, 2, 3, 4, 5, 6, 7, 8, 9, 10, 12, 14, 16 and 24 h), filtered through a 0.45 µm membrane filter and analyzed for drug content by HPTLC at λ_{max} of 250 nm. The cumulative amount of drug permeated through the skin (µg/cm^2) was plotted as a function of time (t) for each formulation. Drug flux (permeation rate) at steady state (Jss) was calculated by dividing the slope of the linear portion of graph with area of diffusion cell. The permeability

coefficient (*K*p) was calculated by dividing *J*ss with initial concentration of drug in donor cell (Co) by using the equation:

$$Kp = Jss/Co \quad (1)$$

The enhancement ratio (*E*r) was also calculated by dividing the *J*ss of respective formulation with *J*ss of control formulation by using the equation:

$$Er = Jss \text{ of SLN formulation}/Jss \text{ of control} \quad (2)$$

3.5.7. In vitro stability at different storage temperature

Short term stability investigations were performed to observe particle growth upon storage of formulations ($BO_{SLN}1$—$BO_{SLN}6$) for a period of 90 days. Initially, particle size and zeta potential measurements were carried out for BO-SLNs. Further, divided into three batches and then kept in colorless and transparent glass vials under different temperature conditions [4 °C (refrigerator), 25 °C (room temperature), and 50 °C (temperature regulated oven)] in black boxes (avoiding interferences). Samples were withdrawn after 90 days for particle size measurements.

Acknowledgement: Authors are thankful to Dr. Sayeed Ahmad, Deptt. of Pharmacognosy and Phytochemistry, Hamdard University, New Delhi, India, for their valuable supports in carrying out this research.

References

Ali J, Akhtar N, Sultana Y, Baboota S, Ahmad S (2008) Thin-layer chromatographic analysis of psoralen in babchi (*Psoralea corylifolia*) oil. Acta Chromatogr 20: 277–282.

Anderson TF, Voorhees JJ (1980) Psoralen photo-chemotherapy of cutaneous disorders. Annual Rev Pharmacol Toxicol 20: 235–257.

Asmussen B (1991) Transdermal therapeutic systems: actual state and future developments. Methods Find Exp Clin Pharmacol 13: 343–351.

Baboota S, Al-Azaki A, Kohli K, Ali J, Dixit N, Shakeel F (2007) Development and evaluation of a microemulsion formulation for transdermal delivery of terbinafine. PDA J Pharm Sci Technol 61: 276–285.

Chang L (2006) Psoriasis Phototherapy: UVA Beats UVB. *WebMD Medical News Daniel De Noon*, July 18.

Craig DQM, Barker SA, Banning D (1995) An investigation into the mechanisms of self-emulsification using particle size analysis and low frequency dielectric spectroscopy. Int J Pharm 114: 103–110.

Farber EM, Nall ML (1974) The natural history of psoriasis in 5,600 patients. Dermatologica 148: 1–18.

Freitas C, Müller RH (1998) Effect of light and temperature on zeta potential and physical stability in solid lipid nanoparticle (SLN^{TM}) dispersions. Int J Pharm 168: 221–229.

Hearst JE (1981) Psoralen photochemistry and nucleic acid structure. J Invest Dermatol 77: 39–44.

Hu FQ, Jiang SP, Du YZ, Yuan H (2005) Preparation and characterization of stearic acid nanostructured lipid carriers by solvent diffusion method in an aqueous system. Coll Surf B: Biointerface 45: 167–173.

Hu FQ, Jiang SP, Du YZ, Yuan H, Ye YQ, Zeng S (2006) Preparation and characteristics of monostearin nanostructured lipid carriers. Int J Pharm 314: 83–89.

Jayaraman K, Velayutham A, Vobalaboina R, Venkateswarlu, Rao YM (2009) Lipid nanoparticles for transdermal delivery of flurbiprofen: formulation, *in vitro*, *ex vivo* and *in vivo* studies. Lip Healt Disease 8: 1–15.

Jenning V, Thunemann AF, Gohla SH (2000) Characterization of a novel solid lipid nanoparticle carrier system based on binary mixtures of liquid and solid lipids. Int J Pharm 199: 167–177.

Lander R, Manger W, Scouloudis M, Ku A, Davis O, Lee A (2000) Gaulin homogenization: A mechanistic study. Biotechnol Prog 16: 80–85.

Lawrence MJ, Rees GD (2000) Microemulsion based media as novel drug delivery systems. Adv Drug Deliv Rev 45: 89–121.

Leite VC, Santos RF, Chen LC (2004) Psoralen derivatives and longwave ultraviolet irradiation are active *in vitro* against human melanoma cell line. J Photochem Photobiol B: Biology 76: 49–53.

Li P, Ghosh A, Wagner RF, Krill S, Joshi YM, Serajuddin ATM (2005) Effect of combined use of nonionic surfactant on formation of oil-in-water microemulsions. Int J Pharm 288: 27–34.

Lippacher A, Müller RH, Mäder K (2002) Semisolid SLN dispersions for topical application: Influence of formulation and production parameters on viscoelastic properties. Eur J Pharm Biopharm 53: 155–160.

Lippacher A, Müller RH, Mäder K (2004) Liquid and semisolid SLN^{TM} dispersions for topical application: Rheological characterization. Eur J Pharm Biopharm 58: 561–567.

Lowe NJ, Chizhevsky V, Gabriel H (1997) Photo (chemo) therapy: general principles. Clin Dermatol 15: 745–52.

Mehnert W, Mäder K (2001) Solid lipid nanoparticles–production, characterization and applications. Adv Drug Deliv Rev 47: 165–196.

Miglietta A, Cavalli R, Bocca C, Gabriel L, Gasco MR (2000) Cellular uptake and cytotoxicity of Solid Lipid Nanospheres (SLN) incorporating doxorubicin or paclitaxel. Int J Pharm 210: 61–67.

Müller RH, Lucks JS (1996) Arzneistoffträger aus festen Lipidteilchen, Feste Lipidnanospharen (SLN). European Patent EP 0605497.

Musajo L, Bordin F, Bevilacqua R (1967) Photoreactions at 3655 Å linking the 3-4 double bond of furocoumarins with pyrimidine bases. Photochem Photobiol 6: 927–931.

Perez C, Castellanos IJ, Costantino HR (2002) Recent trends in stabilizing protein structure upon encapsulation and release from biodegradable polymers. J Pharm Pharmacol 54: 301–313.

Shafiq S, Shakeel F, Sushma T, Farhan JA, Khar RK, Ali M (2007a) Design and development of ramipril nanoemulsion formulation: *in vitro* and *in vivo* assessment. J Biomed Nanotechnol 3: 28–44.

Shafiq S, Shakeel F, Talegaonkar S, Ali J, Baboota S, Ahuja A, Khar RK, Ali M (2007b) Formulation development and optimization using nanoemulsion technique: A technical note. AAPS Pharm Sci Tech 8: E28.

Siekmann B, Westesen K (1994) Melt-homogenized solid lipid nanoparticles stabilized by the nontonic surfactant tyloxapol 1. Preparation and particle size determination. Pharm Pharmacol Lett 3: 194–197.

Zouboulis CC (2004) Acne and sebaceous gland function. J Clin Dermatol 22: 360–366.